Journal of Archaeological Science 64 (2015) 1–11

Contents lists available at ScienceDirect

Journal of Archaeological Science

journal homepage: http://www.elsevier.com/locate/jas

Optically stimulated luminescence (OSL) dating and spatial analysis of geometric lines in the Northern Arabian Desert

C.D. Athanassas [a, *], G.O. Rollefson [b], A. Kadereit [c], D. Kennedy [d], K. Theodorakopoulou [e], Y.M. Rowan [f], A. Wasse [g]

[a] *CEREGE, UMR CNRS-Aix Marseille Université 6635, Technopôle de l'Arbois BP 80, 13545 Aix-en-Provence Cedex 4, France*
[b] *Department of Anthropology, Whitman College, Walla Walla, WA 99362, USA*
[c] *Institute of Geography, Heidelberg University, Heidelberg D-69120, Germany*
[d] *Department of Classics and Ancient History, University of Western Australia, Crawley, WA 6009, Australia*
[e] *Faculty of Geology and the Geoenvironment, University of Athens, Ilissia, 15784 Athens, Greece*
[f] *Oriental Institute, University of Chicago, Chicago, IL 60637, USA*
[g] *University of East Anglia, Norwich NR4 7TJ, UK*

ARTICLE INFO

Article history:
Received 18 June 2015
Received in revised form
9 September 2015
Accepted 18 September 2015
Available online 21 September 2015

Keywords:
Stone structures
Neolithic
Jordan
Wheels
OSL
Quartz
Pattern analysis

ABSTRACT

In this paper we generate chronological constraints through optically stimulated luminescence (OSL) dating on extensive prehistoric stone structures that stretch out in the Arabian Desert and appear as geometric lines, known as the "Works of the Old Men". Two major types of the "Works" that are common throughout the Arabian Desert are the "wheels" and the more intensively investigated "desert kites". Here, OSL dating was applied to "wheels" in the Wadi Wisad area, in the eastern badia of Jordan. OSL dating generated ages that fall into the Late Neolithic to Chalcolithic and Early Bronze Age periods. This chronological spectrum is consistent with the well-documented prehistoric activities at the archaeological site of Wisad Pools, also located in the Wadi Wisad area. Spatial analyses of the "Works" in Wadi Wisad and in the Azraq Oasis revealed that: 1) the wheels are organized in clusters, 2) the spatial distribution of the wheels is predetermined by the kites, 3) the kites were most probably created earlier than the wheels in the study areas and 4) a cluster of wheels nearby the Azraq Oasis tentatively demonstrates ranking and, perhaps, tendency for alignment, although this is not the case for the other wheel-clusters studied. Despite the progress toward understanding the chronological and spatial aspects of the wheels, a great deal of research remains to resolve the actual nature of these enigmatic stone structures.

1. Introduction

Soon after the Arab Revolt (1916) pilots of the Royal Air Force witnessed, during their regular flights between Cairo and Baghdad, extensive geometric lines running across the Black Desert of Jordan (Maitland, 1927). These features, collectively named by the Bedouin tribes as the "Works of the Old Men" (Maitland, 1927; Rees, 1929), are not restricted to the northern Arabian Desert but occur throughout the entire Arabia region, from Syria across Jordan and Saudi Arabia to Yemen, as aerial and satellite imagery proved later (Kennedy and Bewley, 2009; Kennedy, 2011 and references therein).

They are more likely to be seen on the great basaltic plateaus of Arabia (*harra* in Arabic) than in claypans (*qa'a*), and with higher incidence in the Harrat ash Sham region, i.e. the great lava field stretching from southern Syria to NW Saudi Arabia. The most startling thing about the "Works" is that they are difficult to identify from the ground. This stands in contrast to their apparent visibility from the air. In addition, they demonstrate specific geometric patterns (Fig. 2) and extend from a few tens of meters up to several kilometers, evoking parallels to the well-known system of geometric lines of Nazca, Peru.

The "Works" are entirely made out of the basaltic rock of the harrats (plural of *harra*), the standing remains of which are today seen as stacks of 2 or 3 slabs. They are classified in four main categories based on their shape as seen from above (Kennedy, 2011; Kennedy et al., 2014) and correspond to "kites", "meandering walls", "wheels" and "pendants". Kites are extensive (i.e. several

* Corresponding author.
E-mail addresses: athanassas@cerege.fr, athanassasc@gmail.com (C.D. Athanassas).

http://dx.doi.org/10.1016/j.jas.2015.09.005
0305-4403/

Fig. 1. Snapshot of the Middle East, including the study areas. (Base map from ArcGIS. Source: Esri, DigitalGlobe, GeoEye, Earthstar Geographics, CNES/Airbus DS, USDA, USGS, AEX, Getmapping, Aerogrid, IGN, IGP, swisstopo, and the GIS User community).

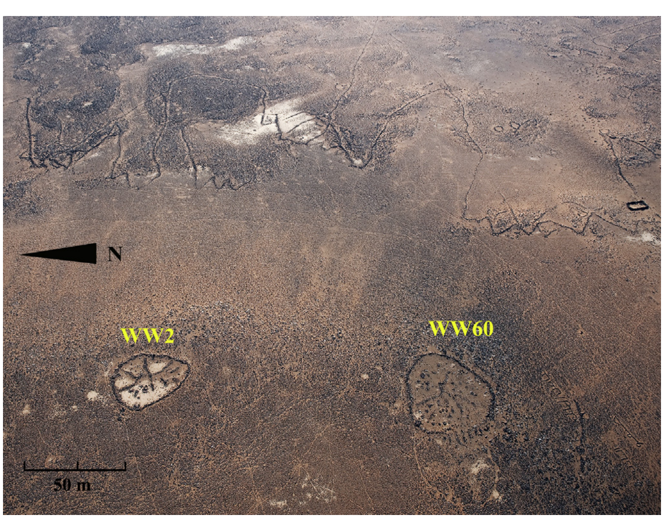

Fig. 2. The "Works of the Old Men" at Wadi Wisad: the studied wheels and a meandering wall to the east. (Aerial photograph by D. Kennedy).

hundred-meters up to kilometers long) stone structures (Fig. 3) named after their resemblance to the kites used for recreation. Several possible functions for the kites have been suggested, from cultic to herding, with the latter seeming as the most likely (cf. Zeder et al., 2013). Kites would funnel large fauna and trap it into an enclosure for slaughtering (Zeder et al., 2013). Little is known about the use of meandering walls. However, they frequently appear as part of the kite system, probably used for "stock herding and control" (Kennedy, 2012). The wheels constitute circular stone arrangements with spokes radiating out of an approximate center. Their function is the subject of debate: although initially proposed to be a type of prehistoric settlement (Kempe and al-Malabeh, 2010, 2013), examination of variants on the basic style challenge that speculation in favor of funerary or ritual use (Kennedy, 2011), as suggested by sepulchral cairns that are enclosed by or encompass the wheels. Pendants (arrays of cairns) frequently intermingle among the other types of the "Works".

Evidence for chronometric dating is rarely unambiguous with the "Works". The established concept that the oldest kites date back to the 7th millennium BCE is the product of association with artifacts of familiar typology, or through correlation with adjacent structures where ^{14}C dating on archaeological remains was feasible (c.f. Betts, 1999; Helms and Betts, 1987; Kennedy, 2011). Recently,

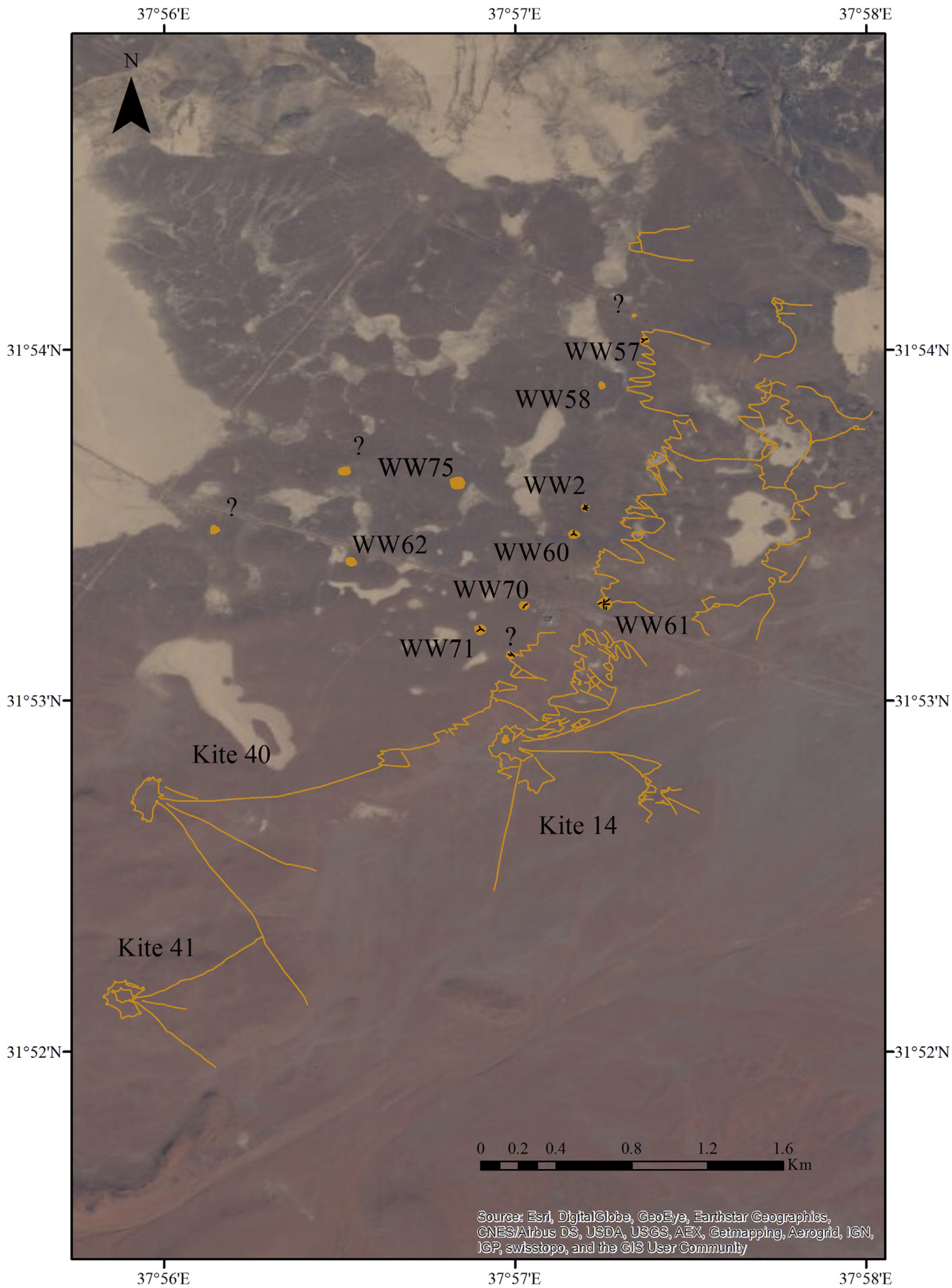

Fig. 3. The system of the "Works" at Wadi Wisad. The excavation site is to the NE, out of the satellite window (source same as Fig. 1). Feature labeling after APAAME (Aerial Photographic Archive for Archaeology in the Middle East). Question marks show wheels to be listed by APAAME.

Zeder et al. (2013) compiled published dates for different kites demonstrating that the kites of the region were being in use as late as the second millennium BCE.

Optically stimulated luminescence (OSL) dating is capable of overcoming obstacles caused by the lack of datable organic material because it can directly date the silicate mineralogical content of sedimentary deposits, be they natural or anthropogenic. In addition to sediment dating, OSL is capable of estimating the age of architectural remains (Liritzis, 2011), as the rapid resetting of the OSL signal in daylight guarantees accurate assessment of the time elapsed since the last exposure of the ground surface or the overlying rock surfaces to daylight. Applications of OSL to the dating of geometric lines so far have been few but effective, designed specifically for the dating of the Nazca lines in the Peruvian Desert (Rink and Bartoll, 2005; Greilich et al., 2005; Greilich and Wagner, 2006). More recently, Holzer et al. (2010) worked out constraints on the chronology of kites from the Judean Desert using OSL dating as well.

Here we provide, through OSL dating, the first framework of numerical ages for the less understood class of the “Works” - the wheels - by analyzing a group of these features at Wadi Wisad, an area of archaeological interest in the eastern badia region of Jordan (Fig. 1). Further, spatial statistics was employed to throw light on the topological aspects of the wheels, and specifically on their topological relations with the kites and local water resources, on their spatial arrangement (clustering), and finally on possible alignments encoded in their design. Such a question was posed for the bearings of the pendant tails (Kennedy and Bishop, 2011) and the alignments of a special type of wheel in Saudi Arabia (Kennedy, 2011). For this reason the sparse records from Wadi Wisad were combined with a larger dataset from the “Works” of the Azraq Oasis (Qa'a el-Azraq), which exhibits one of the densest systems of geometric lines in Harrat ash Shaam (Helms and Betts, 1987; Kennedy, 2011).

2. Study area, materials and sample sites

Wadi Wisad is mainly known for the prehistoric necropolis and colony of Wisad Pools in the eastern badia of Jordan, east of the Black Desert, ~100 km west of Iraq and almost right on the border with Saudi Arabia. Wisad Pools, currently being excavated by Whitman College and University of Chicago, was once settled by a population of hunting pastoralists who exploited the region from the Late Neolithic to the Early Bronze Age (Rollefson et al., 2010, 2014; Rowan et al., 2015a,b). The settlement is developed on both sides of a wadi and is abundant in structures such as tower tombs, cairns, animal pens and residential dwellings.

The site is also known for a primitive dam system developed by the prehistoric inhabitants to collect rain water in a network of pools, probably during a wetter phase of the Neolithic period (Edgell, 2006). About 3.25 km SW of the ongoing excavation site (Rollefson et al., 2010, 2014; Rowan et al., 2015a,b) lies a system of “Works” which, at the scale of Fig. 3, mainly consists of kites, wheels and meandering walls.

Wadi Wisad cuts through a plateau at an average elevation of 700–750 m, characterized by a remarkably smooth topography. Stray, boulder-sized, basaltic slabs on top of an alluvium form a desert pavement (Anderson et al., 2002; Khresat and Qudah, 2006). The alluvium, developed during former humid geological periods (Edgell, 2006), incorporates basaltic slabs strewn within a finer matrix of mainly sands and lesser amounts of clay and carbonates, but the upper parts of the profile appear thoroughly unconsolidated. The scouring effect of the desert wind has resulted in the exhumation of the basaltic slabs from the weathering profile to form the desert pavement (Allison et al., 2000). The majority of the sediments in the eastern badia are rich in quartz, blown from southerly sources (Allison et al., 2000), like Wadi Rum and Wadi Araba deserts in southern Jordan, and northern Saudi Arabia.

The “Works” were constructed by stacking the basalt slabs that litter the desert area one onto another (Fig. 4a), exposing the light-hued underlying sandy or gritty substratum of the desert. The local basalt does not exhibit macroscopically visible feldspar crystals, and therefore direct dating of the stone surfaces using high-resolution optically stimulated luminescence (HR-OSL, cf. Greilich et al., 2005; Greilich and Wagner, 2006; Rhodius et al., 2015) is not possible (Kadereit et al., 2008). As the mafic volcanic rocks do not contain coarse quartz grains we could not follow the approach of stone-surface dating of Simms et al. (2011) either. As these methods of directly dating the construction of the wheels were not possible, we took advantage of the fact that the sediment beneath the boulders is rich in quartz.

On the assumption that any luminescence signal of sand-sized quartz in the ground surface was totally erased before the placement of the basaltic slabs, OSL dating of quartz from the ground surface underlying the arrays of slabs would provide a maximum age for the structure (Holzer et al., 2010). However, the uppermost part of the unconsolidated sediments would always be agile in this wind-dominated environment, and their luminescence thoroughly zeroed at any time. Therefore, placement of a stone on top would preserve that sediment. Although it is a kind of indirect dating for the stone work, OSL dating of the underlying sediment would result in an OSL age equivalent to the age of the construction of the wheels.

Fig. 4. a) Appearance of the wheels at Wadi Wisad at ground level. b) Photograph showing the sampled sediment underneath a toppled basaltic slab at WW2. White color corresponds to spray paint delineating the boundary of the slab. Photograph taken in the morning after sample collection.

Samples were collected from two of the wheels cropping out at Wadi Wisad (WW2 and WW60 in Fig. 3). Suitable slabs on the perimeter of the wheels were marked out in daytime by spray-paint (Fig. 4) and toppled at night to avoid exposing the underlying material to sunlight. A ~ 1 cm thick film of sediment from underneath the slab was swiped into a dustpan from each sample spot. Seven samples were collected well before sunrise (4 from WW2 and 3 from WW60), and were immediately sealed in opaque wrapping. One of the samples (WW2-4) comes from underneath a slab of a cairn contained within wheel WW2. Along with the underlying sediment the basaltic slab was also sampled for dosimetric purposes.

3. OSL dating

OSL dating of the Wadi Wisad wheels took advantage of the

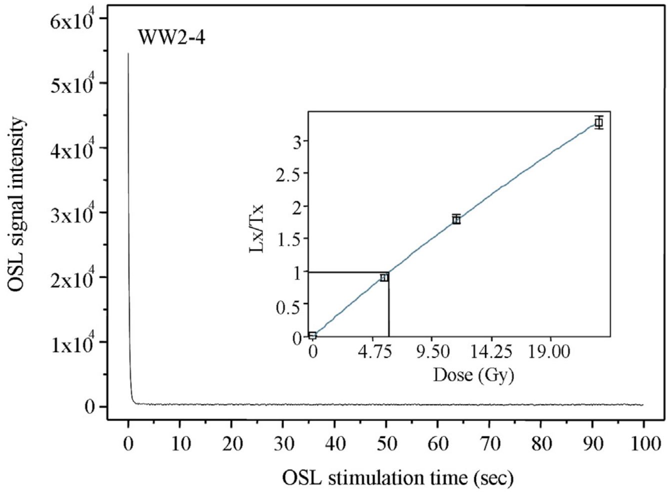

Fig. 5. Decay curve of a sample from Wadi Wisad wheel No 2 (left), and its associated growth curve (insert right). Recycling point at 6.3 Gy. Unit on Y-axis for the decay curve is counts/sec.

quartz content in the sampled sediments. Preference for quartz to feldspar, the other routinely used mineral in luminescence dating, was justified for that OSL from quartz remains stable over extremely long geological timescales, while any inherent latent luminescence is assumed to rapidly zero (bleaching) before deposition during aeolian transportation (Duller, 2004). Samples were processed at the Heidelberg Luminescence Laboratory. Pure quartz was obtained after 1) treatment with acetic acid for carbonates removal, 2) hydrogen peroxide for organic materials removal, 3) mechanical sieving to separate 125–212 μm grains, 4) density separation to isolate coarse quartz from other minerals, and 4) hydrofluoric acid etching to remove the outer rim of the quartz grains influenced by alpha radiation from the surrounding sediment. The preparation procedure is described in detail in Kadereit et al. (2006, 2008).

An OSL age based on the quartz content of a sediment is the ratio of the total radiation dose delivered to the quartz grains from the surrounding geological materials, over the rate it was delivered, the latter known as the “dose rate”. Optically stimulated luminescence's intensity decays with the stimulation time (decay curve in Fig. 5), and its integral is proportional to the dose. The laboratory dose equivalent to that delivered in nature, termed the “equivalent dose” (D_e), can be evaluated by interpolating the natural OSL signal intensity of a single aliquot onto a regression formula, mostly linear or single exponential, that represents the best fit to an empirical correlation containing pairs of known doses (regenerated doses) with their associated OSL signal intensities, the latter normalized by a constant dose (test dose). The resulting plot is termed the “growth curve” (inset in Fig. 5). This measurement procedure summarizes the standard single aliquot regenerated protocol by Murray and Wintle (2000).

For the dose rate estimation we assumed contribution from both the overlying basalt slab that is in physical contact with the sampled grains and the underlying sediment. Therefore, the actual dose rate on the sampled grains at the interface should be equal to the average of the basalt dose rate and the underlying sediment dose rate (Chapot et al., 2012).

Material from both the basalt slabs and the sediment were submitted to radioelemental analysis by means of ICP-MS (Acme-Labs, BC, Canada). U (ppm), Th (ppm) and K (wt %) concentrations were converted to dose rates, listed in Table 1, using conversion factors by Guérin et al. (2011). For the samples from the plateau no correction was necessary for potential topographic shielding of the cosmic radiation. Water content was non-existent in the sediments of this hyperarid environment.

Pure quartz was split into several aliquots per sample (~25–45), prepared by mounting 125–212 μm grains onto aluminum cups using silicon oil, sprayed onto the cups through a 2 mm-aperture mask (small aliquots). A RISØ TL-DA-20 luminescence reader, supplied with blue (470 Δ 30 nm) and infrared emitting diodes was employed for the luminescence measurements. An EMI9635Q photomultiplier, a 7.5-mm Hoya U-340 filter and a $^{90}Sr/^{90}Y$ beta source for automated irradiations, delivering 0.095 Gy/sec, were affixed to the luminescence reader.

The SAR method requires repetitive heating, optical stimulation and dosing which may alter the sensitivity (luminescence capacity) of quartz grains in the course of a measurement cycle (cf. Table 2).

Table 1
Elevation, radioelemental concentrations, partial and average dose rates, equivalent doses and OSL ages.

Sample	Elevation (masl)	U sediment (ppm)	Th sediment (ppm)	K sediment (wt %)	Dose rate sediment (Gy/ka)	U basalt (ppm)	Th basalt (ppm)	K basalt (wt %)	Dose rate basalt (Gy/ka)	Dose rate average (Gy/ka)	De (Gy)	OSL age (ka)
WW60-1	720	0.62	2.1	0.20	0.81 ± 0.01	0.3	0.9	0.10	0.55 ± 0.01	0.68 ± 0.01	5.49 ± 0.50	8.08 ± 0.73
WW60-2	720	0.56	1.2	0.14	0.67 ± 0.01	0.3	0.9	0.10	0.55 ± 0.01	0.61 ± 0.01	5.16 ± 0.61	8.46 ± 1.00
WW60-3	720	0.64	2.0	0.24	0.84 ± 0.01	0.3	0.9	0.10	0.55 ± 0.01	0.70 ± 0.01	5.30 ± 0.49	7.57 ± 0.70
WW2-1	720	0.46	1.9	0.21	0.76 ± 0.01	0.3	1.0	0.10	0.57 ± 0.01	0.67 ± 0.01	4.01 ± 0.46	5.99 ± 0.69
WW2-2	720	0.44	2.0	0.22	0.77 ± 0.01	0.2	1.0	0.10	0.53 ± 0.01	0.65 ± 0.01	3.52 ± 0.38	5.42 ± 0.59
WW2-3	720	0.37	1.5	0.18	0.68 ± 0.01	0.3	1.0	0.11	0.57 ± 0.01	0.63 ± 0.01	3.49 ± 0.20	5.54 ± 0.32
WW2-4	720	0.50	2.1	0.26	0.83 ± 0.01	0.3	1.0	0.11	0.57 ± 0.01	0.70 ± 0.01	5.99 ± 0.41	8.55 ± 0.58

Table 2
The single aliquot regenerated (SAR) dose protocol for conventional OSL dating of quartz (Murray and Wintle, 2000). PH corresponds to “preheat”.

Step	Treatment	Measurement	Comment
1	Dose D_i	–	Apply regenerated dose (no irradiation before measurement of the natural signal)
2	PH (240 °C, 10 s)	–	Thermally remove charge from geologically unstable traps
3	OSL 240 °C, 10 s)	L_{OSL}	Register OSL signal (at elevated temperature so as to maintain unstable traps inert)
4	Test Dose T_D	–	Apply test dose
5	PH (160 °C, 0 s)	–	Thermally remove charge from geologically unstable traps
6	OSL (125 °C, 100 s)	T_{OSL}	Register test dose signal
7	Go to Step 1	–	Repeat run using a new regenerated dose

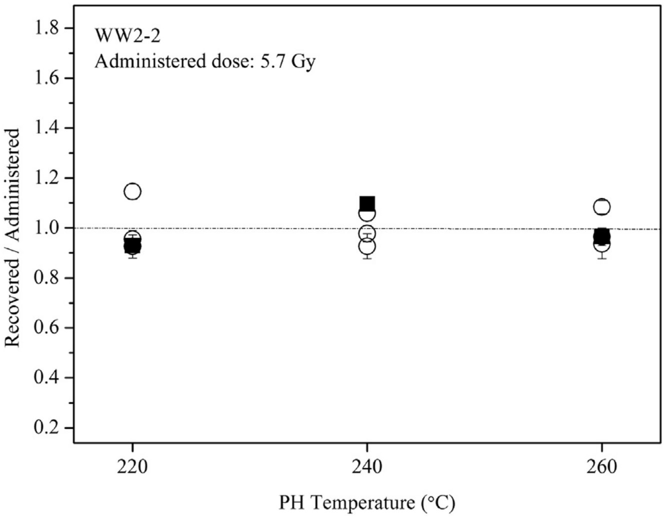

Fig. 6. Preheat test. Aliquots were dosed with 5.7 Gy and measured in sets of 3 at increasing preheating temperatures. Open circles correspond to ratios of individual aliquots and black rectangles to the average ratio at each PH temperature.

Therefore measurement of a constant dose, the "test dose", is repeated throughout the regeneration procedure to monitor and correct for sensitivity changes. Replicate runs of the standard SAR protocol (Table 2) on a sizable set of aliquots per sample enables replicate estimates for the equivalent dose. A typical natural OSL signal (decay curve) and its associated growth curve are shown in Fig. 5. Quartz from Wadi Wisad has the advantage of very bright OSL signals (high signal-to-noise ratios). The associated growth curves are best fitted by a slightly curved single exponential formula, (practically) appearing as almost linear.

The internal reliability of the D_e that can be obtained with the SAR protocol can be supervised by testing the extent to which sensitivity changes can be kept under control (Murray and Wintle, 2000). Sensitivity changes were monitored here a) by a combined dose recovery/preheat (PH) test in which SAR was run on quartz aliquots, artificially bleached (Jacobs et al., 2006a,b) and irradiated with a known dose (5.7 Gy, chosen as being close to the expected D_e), across different PH temperatures (Fig. 6) in order to select the temperature (denoted by the presence of a plateau) that recovers most accurately the dose, and then b) through the recycling ratio that is determined by the quotient of the normalized luminescence responses of duplicate doses at a "recycling point".

Fig. 6 demonstrates independence of the D_e from the preheat temperature (PH), as suggested by the presence of a plateau between 220 °C–260 °C, therefore rendering 240 °C as an appropriate PH temperature. At the PH temperature of 240 °C, 95% of the aliquots measured per sample yielded recycling ratios diverging less than 10% from unity, suggesting that the measurement settings shown in Table 1 are appropriate for controlling sensitivity changes and for measuring the D_e accurately (Murray and Wintle, 2000). Aliquots with recycling ratios falling outside the 10% tolerance interval from unity (Murray and Wintle, 2000) were excluded from the calculations.

Equivalent doses can be graphically displayed by radial plots (Fig. 7), here created using the computer software *RadialPlotter 7.2* (Vermeesch, 2009). Radial plots (Galbraith et al., 1999; Galbraith

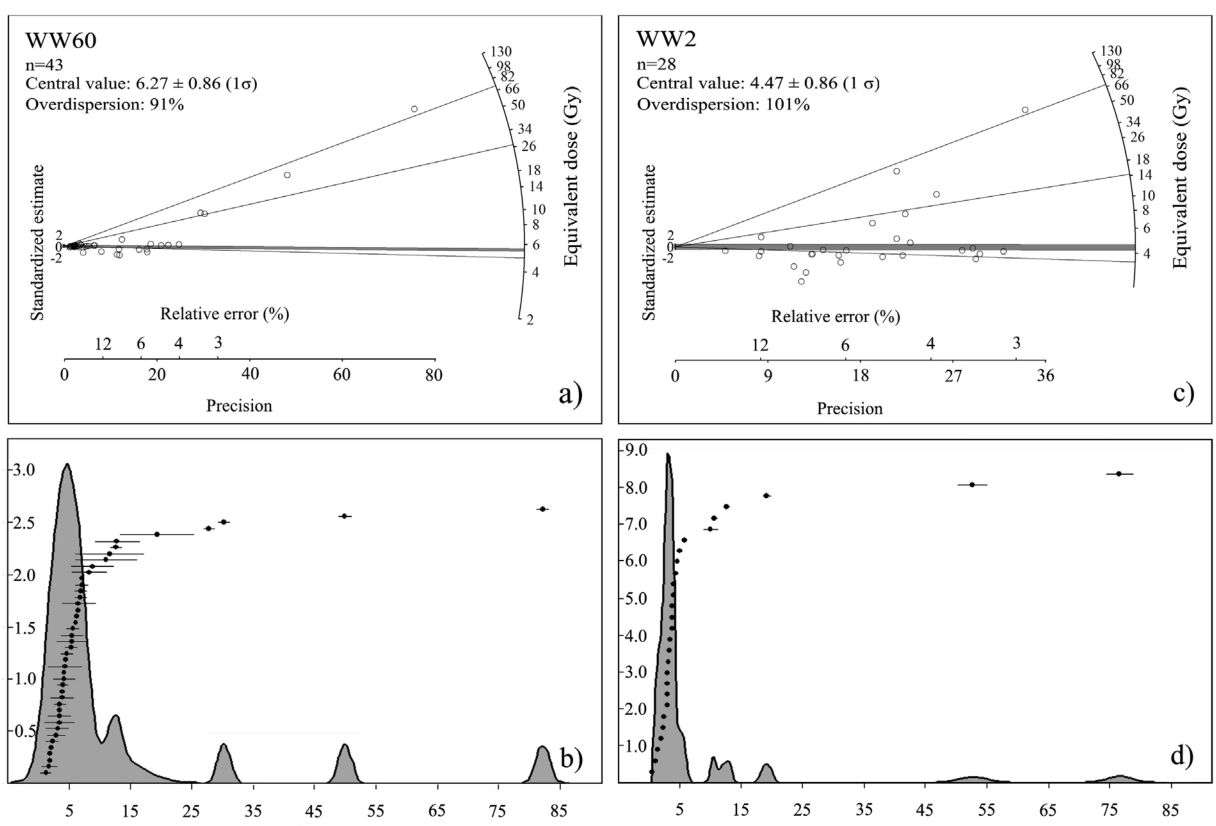

Fig. 7. Representative radial plots for samples WW60 and WW2 (a and c) and their corresponding probability density plots (b and d) underneath. Unit on Y-axis for b) and d) is probability.

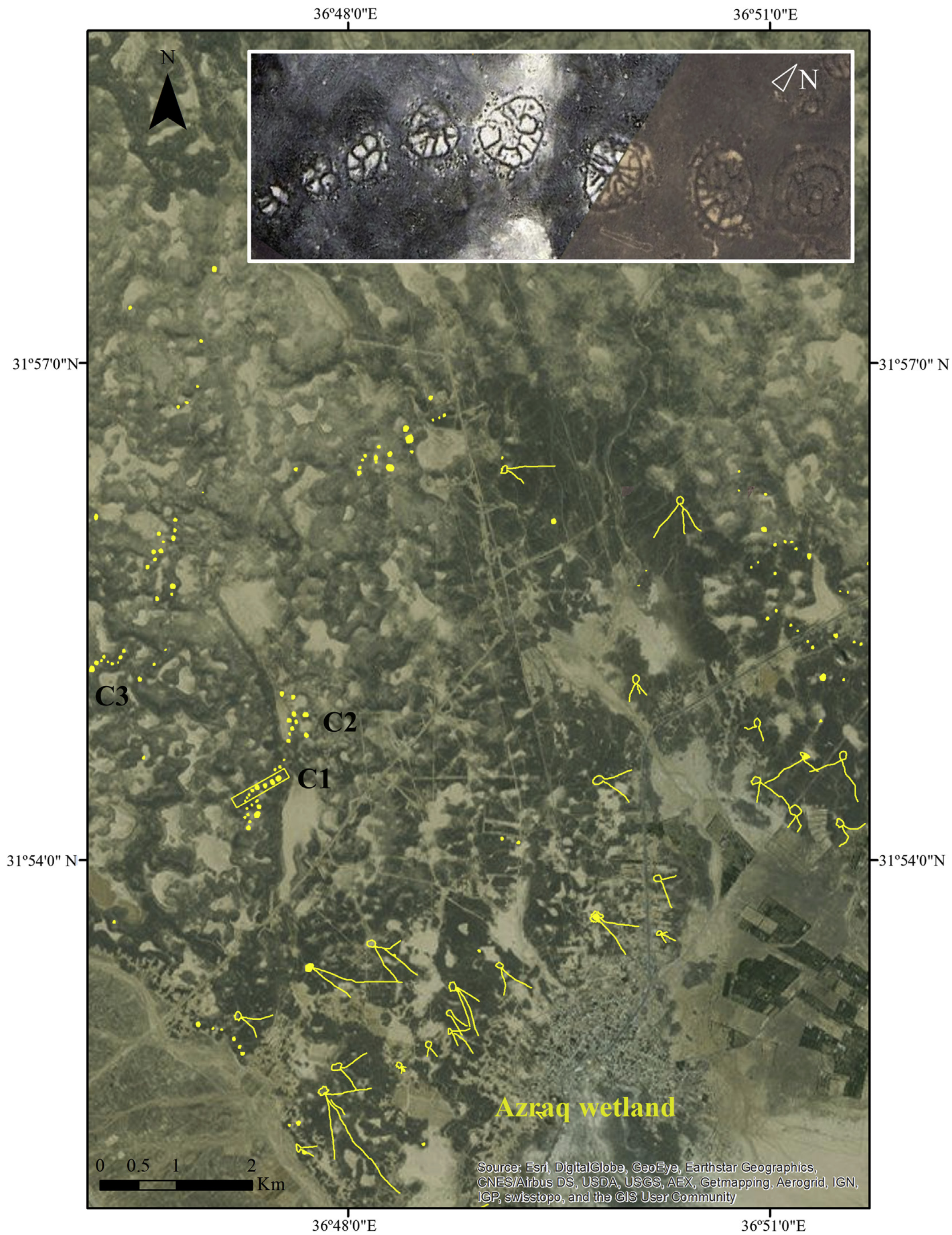

Fig. 8. The satellite observation window offered for Qa'a el-Azraq and the surrounding harra. Wheels are illustrated as yellow spots beyond the traps of kites. In the rarest occasion where potentially remodeled wheels tended to morphologically overlap with animal pens the spot was left blank. The small rectangle at center-left outlines Azraq cluster 1, expanded in the top-right inset. (source of base-map as Fig. 1).

and Roberts, 2012) are scatter plots of the individual standardized D_e estimates versus the inverse squares of their standard errors; the higher the precision, i.e. the smaller the appended standard error, of a D_e is, the more to the right along the horizontal axis the D_e value appears. Therefore, radial plots permit direct comparisons between D_e estimates that are subject to variable errors, while presenting a comprehensive picture of the overdispersion. Radial plots (Fig. 7a,c) are centered on a central value (representing the average D_e) enveloped in a 95% confidence interval ($\pm 2\sigma$ band, gray strip).

Representative examples of samples from the study area are given in Fig. 7a,c. These illustrate that the D_e estimates are hardly concordant with the central value (within the 95% confidence interval), suggesting that the spread may be the result of mixed populations, each with different D_e values (Galbraith and Roberts, 2012). The corresponding probability density plots (Fig. 7 b,d) support the visual impression of multiple populations as they clearly illustrate a dominant and sharp peak emerging at ~5 Gy, set well apart from outliers toward the upper end of the D_e spectrum.

It has been demonstrated (c.f. Roberts et al., 2000; Jacobs et al., 2006a,b; 2008) that it is possible to statistically separate mixing populations with different doses and to accurately assess the D_e for each population. By applying a finite mixture model using *Radial-Plotter* it was possible to identify three populations of equivalent doses in each sample (radii in Fig. 7a, c), with the predominant population (~85% of the dataset) consistently peaking within the interval 3.5–5 Gy and the remainder ~ 10% and ~5% of the dataset systematically pointing at much larger doses (~20 Gy and ~70 Gy) respectively.

Given the average dose rate (Table 1) it becomes evident that the smaller populations clustering around the larger dose peaks are beyond the archaeological context of the "Works" as they would intimate "Pleistocene ages", which is an absurd conclusion.

Ruling out poor signal resetting in airborne quartz sand, and undermining the possibility of substantially inhomogeneous dosimetry (see similar dose rates of basalt slabs and underlying sediment in Table 1), we are inclined to attribute the apparent dispersion of D_e values to minor mixing due to limited and accidental turbation during sampling with grains from deeper into the alluvium containing larger doses, and regard the prevalent cluster of smaller equivalent doses suitable for the OSL dating of the construction of the wheels in Wadi Wisad.

D_e estimates were obtained for each sample by applying the central age model (CAM) of Galbraith et al. (1999), not to the whole D_e population but only to the predominant cluster of lower equivalent doses. D_e estimates, OSL ages and their standard errors are shown in Table 1.

4. Spatial analysis

Archaeological sites may be regarded as "open systems"; information is exchanged between archaeological features, or between the features and their enveloping landscape. Therefore, spatial analysis may illuminate certain queries regarding the topology of the "Works" in the eastern badia, that is the spatial relationships between the features and their surrounding landscape, and relationships among the features themselves.

Here we address three issues of the spatial properties of the "Works" with respect to (1) the pattern of exploitation of the surrounding environment and the topological relationships between the kites and the wheels; (2) the spatial distribution of the wheels over the desert terrain and (3) possible orientations in the design of the wheels that may reflect specific prehistoric perceptions and functions.

In order to overcome the limited observation window offered for Wadi Wisad by the available satellite imagery (Fig. 3), and take advantage of a larger dataset, spatial analysis extends beyond the dated sites in the eastern badia to also include the cognate system of geometric lines at the Azraq Oasis, which abounds in "Works" of all the types mentioned above. The "Works" at Azraq Oasis (as well as for Wadi Wisad) were digitally extracted on vector layers by tracing them on the ArcGIS satellite base-map. We extracted the vector outline of 199 wheels and 46 kites from a 26 km × 26 km window around the Azraq Oasis. Spatial analysis and statistical processing of the spatial datasets were carried out using *ArcGIS* 10.2.2 and *MATLAB* R2007b.

1. *Topological aspects of the "Works".*

A first glimpse of the "Works" shown in Fig. 8 reveals that wheels mainly crop out in clusters whereas kites tend to neighbor claypans which, occasionally, fill with shallow rain water. Although the tails of the kites may have been situated in order to cut across the watershed for driving the grazers, the groups of wheels are located entirely on elevated spits of barren basalt that lie between the claypans. Thus, the spatial arrangement of the "Works" (Figs. 3 and 8) seems to unfold in a specific manner, with the kites radiating out of the perimeter of a local water body, either permanent or seasonal (i.e. the wetland at Azraq or the dried-up playas, pools and small wadis east of the Wisad kites respectively), isolating the wheels outside their domain with almost no exception.

The observed order of "water-kites-wheels" comprises a pattern recurring in both areas, even though they are 100–150 km apart. Notably, the wheels never appear mingled among the kites, with the exception of a few cases where the heads of some kites have been remodeled to wheels (Azraq: E36°49′46″/N31°53′40″, E36°51′15″/N31°54′38″, E36°47′43″/N31°53′21″) or wheels have incorporated part of the meandering walls into their perimeter (Wadi Wisad: WW57, WW61 in Fig. 3). Such intersections allow relative chronological stratification of the "Works" to some extent.

2. *Pattern analysis of the wheels*

Standard pattern analysis methods on the wheels, such as average nearest neighbor and multi-distance spatial cluster analysis, were employed to provide a statistical parameterization of the macroscopic observations presented above (Mitchell, 2005). Having calculated the centroids of the wheels (treated as point features), the computed distances linking all possible pairs of nearest centroids yielded an observed mean nearest neighbor distance 0.39 times the expected one (i.e. mean of all distances between possible pairs), generating a z-score of −16.40 which is well out of the [−1.96, 1.96] interval for randomly distributed positions at the 95% significance level. We thus reject the null hypothesis going on to claim that the wheels are indeed spatially distributed as clusters.

Wheels were further investigated to see how clustering varies with the scale of observation. This was done by applying multi-distance spatial cluster analysis that utilizes Ripley's K function. Ripley's k function compares the number of observed neighboring wheel centroids (solid curved line in Fig. 9) at multiple distances to the number of centroids expected from a completely random point

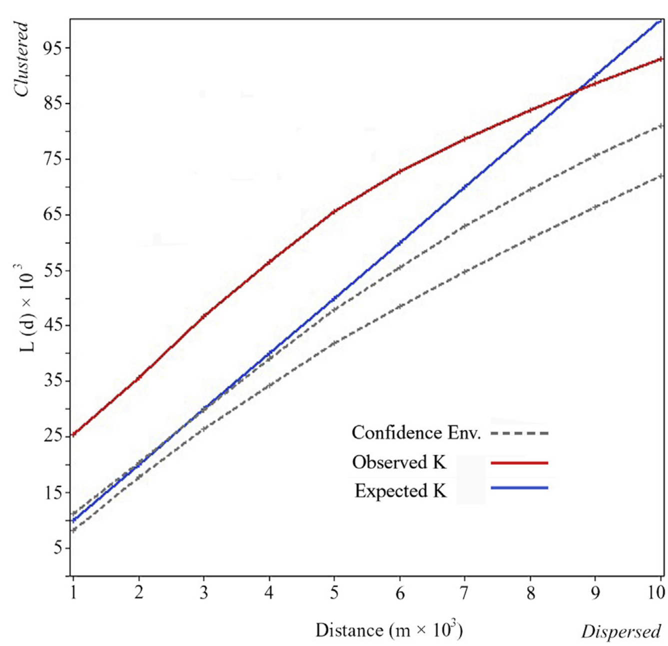

Fig. 9. Multi-distance cluster analysis for wheels of Qa'a el-Azraq. Straight line corresponds to the predicted function of the distribution of positions randomly spread, solid curved line corresponds to the observed function of the distribution of wheels and dashed lines correspond to the confidence levels.

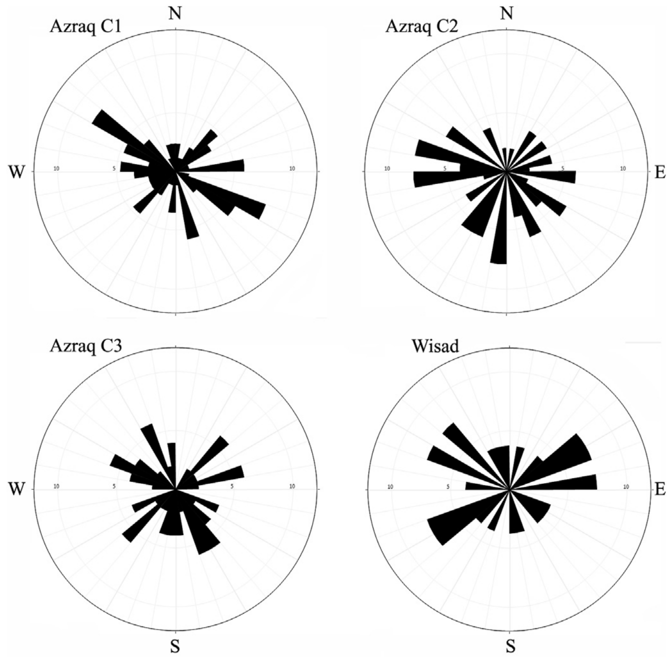

Fig. 10. Rose diagrams for selected clusters of wheels near Azraq Oasis (C1,C2, C3) and Wadi Wisad. Designed by Stereonet (Allmendinger et al., 2013; Cardozo and Allmendinger, 2013).

distribution (straight line in Fig. 9). If the observed number exceeds the predicted one then the pattern is interpreted as clustered, otherwise as dispersed. This is demonstrated in Fig. 9, where the clustered patterning is preserved for a distance of ~9 km and then it depletes towards dispersion.

3. *Orientation of wheel spokes*

A characteristic feature of the wheels is spokes consisting of almost linear arrays of stones striking out of an approximate center in variable directions, giving the impression of radii. In several cases the outline is so accurately circular that the stone spokes indeed correspond to radii. It is reasonable to wonder if their azimuths are distributed in excess in a certain direction, for example with astronomical or physiographic importance to the prehistoric dwellers (e.g. van den Bergh, 1992). If certain azimuths were significant, one would expect the relevant spokes to strike at greater frequency. This query was explored by creating rose diagrams for selected clusters of wheels.

From the rose diagrams of Fig. 10 it becomes evident that there is no common motif of azimuth distribution shared among the tested wheels, nor is there a systematic preference for a certain direction. An exception may occur for cluster C1 from Azraq, where there is a slight predominance of SE–NW directions.

A x^2-test for the randomness of the directional data, sorted into 12 bins of 30° (degrees of freedom $\Phi = 10$), returned measured x^2 of 89.600, 6.1765, 10.4118 and 4.556 for Azraq clusters 1,2,3 and Wisad cluster respectively, and a critical x^2 of 18.3070 at the 95% confidence level. That the calculated x^2 for Azraq cluster C1 is well above the critical x^2 but less than that for the other wheel clusters suggests that the spokes of Azraq cluster C1 are *non-randomly* distributed, whereas the azimuth distribution of the remaining is the result of chance.

5. Discussion and conclusions

The range of OSL dates for the measured sediment underlying the wheels at Wadi Wisad covers the age range 8.55 ka - 5.42 ka within 10–11% standard error. Dating of sediments has constituted a maximum age for the overlying stone structures (Holzer et al., 2010). Nevertheless, aside from the preservation of the sediment underneath a slab, other processes that may occur in stony deserts is the gradual entrainment of aeolian material (vesicular sediment) from the surrounding ground surface into voids of the alluvium underneath the slab, after the emplacement of the slab (Anderson et al., 2002; Dietze and Kleber, 2012; Dietze et al., 2012). Therefore, presence of vesicular sand, blown later in the samples, would challenge the assumption of an equivalent age for the construction event.

D_e distributions show a steep rise at the lower edge (Fig. 7). However, in case of mixed-in sand leading to the formation of a vesicular horizon underneath a slab one would expect a slowly rising limb of D_e values at the lower end of the data distribution. We therefore interpret our data in favor of the equivalent age model (see Section 3), for which it is assumed that the quartz-rich top

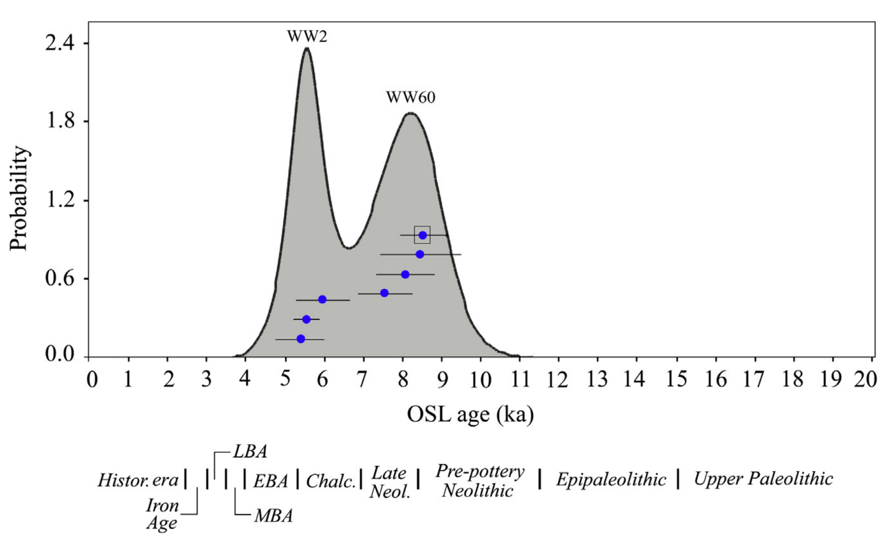

Fig. 11. Distribution of the OSL ages generated for the studied wheels at Wadi Wisad. The ages for the two wheels cluster around the EBA to Chalcolithic (WW2) and Late Neolithic (WW60) periods respectively. Framed-up data point corresponds to the sampled cairn within WW2 (sample WW2-4).

layer at the desert surface, prior to the stone emplacement, was continuously reworked by wind action and thoroughly zeroed at any time, or that any additional aeolian vesicular sediment beneath an intentionally placed basalt slab formed very quickly, i.e. within a time period well within the error margins. Therefore, we consider the OSL ages of the sediment layer as equivalents of the construction of the wheels on top. Taken as a whole, that time-span captures the period of time from the Late Neolithic to the Chalcolithic and the Early Bronze Age (Fig. 11).

Rollefson et al. (2014) and Rowan et al. (2015a) presented a number of ^{14}C dates for the nearby Wisad Pools settlement. Ages of 7690 ± 40 B P. (2σ: 6606–6455 cal BCE), 7620 ± 40 B P. (2σ: 6590–6580 cal BCE), 7010 ± 40 B P. (2σ: 6000–5840 cal BC) and 6730 ± 40 B P. (2σ: 5710–5610 cal BCE) from charcoal retrieved from stratigraphic units excavated within houses at Wisad Pools conform with the OSL chronology. In addition to the technically good behavior of the SAR protocol (see Section 3) and the correspondence of the OSL ages for the wheels with independent age for human activity in the surroundings provides confidence in the here chosen approach of OSL dating. Taking the group of Wisad wheels as a cluster, we can confidently posit a Late Neolithic to Early Bronze Age chronology for the remainder wheels at Wisad as well.

It is striking that the OSL ages cluster in two periods, i.e. around ca. 8.5 ka (WW60) and 5.4 ka (WW2), respectively (Fig. 11). Assuming that the OSL ages represent age equivalents for the date of construction, the oldest OSL ages around ~8.5 ka could point to the earliest time of construction of the wheels, whereas the younger ages could point to a later period of construction, or modification of the wheels around 5.4 ka. More to the point, the cairn sample WW2-4 yielded an age older than the surrounding wheel, matching the age of the older WW6 wheel. That suggests to us that the two wheels were constructed together in the Late Neolithic period but the perimeter of WW2 was remodeled (or repaired) during the EBA to Chalcolithic period, while the prehistoric dwellers knew what that cairn was when working on the wheel, such that they did not removed the stones, and worked around it.

Topological associations revealed that the kites regularly tend to edge between the domain of the wheels and a local water body, whether it is the wetlands around Azraq Oasis or the wadis around Wisad Pools. A similar motif between wheels and kites was also observed in the Safawi area of the Black Desert, east of Azraq (Kennedy, 2012). As the prehistoric population would not obviously allocate space between the wheels and the water body to be later used for the construction of kites, it is suggested that the kites may predate the wheels, as Helms and Betts (1987) speculated. The same conclusion is drawn in cases where the heads of some kites have been remodeled to wheels. This might explain why the kites seem to exclude the wheels out of their domain, probably to eliminate the possibility of physical interference with the wheels.

The combination of OSL dates with the topological relationships outlined above highlights interesting chronological implications for the Wisad kites and the meandering walls (Fig. 3), which seem to be part of the local kite system. Meandering walls meet with wheels WW57, WW61 and a so far unlisted wheel SE of WW71. Such an intersection is unlikely to be the result of chance, thus we assume these specific wheels were made to link the walls and the kites. Such a relationship would render the Late Neolithic as a minimum age for the kites and walls of Wisad. Hints in Sumerian (Gilgamesh Epic) and Akkadian texts for hunting and animal husbandry practices that echo use of kites (Helms and Betts, 1987) intimate that the kites were still functioning long after the Neolithic chronology of the wheels, a conclusion also emerging from Zeder's et al. (2013) compilation of dates for kites.

Spatial statistics on the wheels reveals that they are organized in clusters rather than being randomly distributed. This allows speculation that a common quality is shared among the members of each cluster. The ritual/funerary importance of the wheels (Kennedy, 2011) is frequently hinted at by the sepulchral cairns enclosed within their perimeter, and thus the quality shared among the members associated with the wheels could be ritual in nature as well. Strikingly, one cluster in the vicinity of Azraq Oasis (C1 in Fig. 8) exhibits systematic gradation of the wheel size lengthwise, which is definitely beyond chance, motivating us to wonder if the shared quality also exhibited some sort of ranking in that Late Neolithic-Early Bronze Age society.

No pronounced orientation was found among the tested clusters except for the above mentioned cluster in Azraq that exhibits ranking (C1). The x^2-test showed that the majority of the spokes of the wheels in that cluster are oriented for some reason to stretch in a SE–NW direction. This bearing points at the quartile of the horizon where the sun rises during the winter solstice; that is the dominant orientation of the funerary megalithic structures of the Mediterranean (Hoskin, 2009). Whether this alignment was indeed intended by the prehistoric builders, or owes to a local topographical peculiarity, that can not be identified at the current observation scale, can not be answered at the moment. As for the rest of the wheels, they do not seem to contain any archaeostronomical information.

Although additional research is required to fully elucidate the OSL chronology of the wheels in northern Arabia, the OSL dates from Wadi Wisad and the preliminary inter-site spatial analyses, are a useful step to interpreting their age and use. What we have understood so far is that these features are the product of a long-lasting modification process of the desert by the prehistoric inhabitants that resulted in the characteristic landscape of the “Works”. This immense cultural modification of the desert landscape is the result of collective work with functional and religious importance, a work intended to be used and commemorated for an indefinitely long time.

Acknowledgments

Study of the “Works of the Old Men” in Jordan was funded by the Mistrals-EnviMed program, W.O.MEN (Works of the Old Men), for 2012–2014. We are thankful to Barbara Porter, Director of the American Center for Oriental Research (ACOR), Amman, Jordan, for welcoming this project in Jordan, and the Department of Antiquities of Jordan. Special thanks also to Jutta Asmuth (Heidelberg Luminescence Laboratory) for her assistance during the sample preparation and the measurements. An anonymous reviewer is thanked for their useful comments.

References

Allison, R.J., Grove, J.R., Higgit, D.L., Kirk, A.J., Rosser, N.J., Warburton, J., 2000. Geomorphology of the eastern Badia basalt plateau, Jordan. Geogr. J. 166, 352–370.

Anderson, K., Wells, S., Graham, R., 2002. Pedogenesis of vesicular horizons, Cima volcanic field, Mojave desert, California. Soil Sci. Soc. Am. 66, 878–887.

Allmendinger, R.W., Cardozo, N.C., Fisher, D., 2013. Structural Geology Algorithms: Vectors & Tensors. Cambridge University Press, Cambridge, England, 289 pp.

Betts, A.V.G., 1999. The Harra and the Hamad: Excavations and Surveys in Eastern Jordan. Sheffield Academic Press, Sheffield, p. 240.

Cardozo, N., Allmendinger, R.W., 2013. Spherical projections with OSXStereonet. Comput. Geosci. 51, 193–205. http://dx.doi.org/10.1016/j.cageo.2012.07.021.

Chapot, M.S., Sohbati, R., Murray, A.S., Pederson, J.L., Rittenour, T.M., 2012. Constraining the age of rock art by dating a rockfall event using sediment and rock-surface luminescence dating techniques. Quat. Geochronol. 13, 18–25.

Dietze, M., Bartel, S., Linder, M., Kleber, A., 2012. Formation mechanisms and control factors of vesicular soil structure. Catena 99, 83–96.

Dietze, M., Kleber, A., 2012. Contribution of lateral processes to stone pavement formation in deserts inferred from clast orientation patterns. Geomorphology 139/140, 172–187.

Duller, G.A.T., 2004. Luminescence dating of quaternary sediments: recent advances. J. Quat. Sci. 19, 183–192.
Edgell, H.S., 2006. Arabian Deserts. Nature, Origin and Evolution. Springer p.592.
Galbraith, R.F., Roberts, R.G., Laslett, G.M., Yoshida, H., Olley, J.M., 1999. Optical dating of single and multiple grains of quartz from Jinmium rock shelter, northern Australia: part I, experimental design and statistical models. Archaeometry 41, 339e364.
Galbraith, R.F., Roberts, R.G., 2012. Statistical aspects of equivalent dose and error calculation and display in OSL dating: an overview and some recommendations. Quat. Geochronol. 11, 1–27.
Greilich, S., Glasmacher, U.A., Wagner, G.A., 2005. Optical dating of granitic surfaces. Archaeometry 47, 645–665.
Greilich, S., Wagner, G.A., 2006. Development of a spatially resolved dating technique using HR-OSL. Radiat. Meas. 41, 738–743.
Guérin, G., Mercier, N., Adamiec, G., 2011. Dose rate conversion factors: update. AncientTL 29, 5–8.
Helms, S., Betts, A., 1987. The desert 'kites' of the Badiyat esh-Sham and north Arabia. Paléorient 13, 41–67.
Holzer, A., Avner, U., Porat, N., Kolska Horwitz, L., 2010. Desert kites in the Negev desert and northeast Sinai: their function, chronology and ecology. J. Arid Environ. 30, 1–12.
Hoskin, M., 2009. Orientations of dolmen of Western Europe. Complutum 20, 165–175.
Jacobs, Z., Duller, G.A.T., Wintle, A.G., Henshilwood, C.S., 2006a. Extending the chronology of deposits at Blombos Cave, South Africa, back to 140 ka using optical dating of single and multiple grains of quartz. J. Hum. Evol. 51, 255–273.
Jacobs, Z., Wintle, A.G., Duller, G.A.T., 2006b. Evaluation of SAR proce-dures for De determination using single aliquots of quartz from two archaeological sites in South Africa. Radiat. Meas. 41, 520–533. http://dx.doi.org/10.1016/j.radmeas.2005.10.008.
Jacobs, Z., Wintle, A.G., Duller, G.A.T., Roberts, R.G., Wadley, L., 2008. New ages for the post-Howiesons Poort, late and final middle stone age at Sibudu, South Africa. J. Archaeol. Sci. 35, 1790–1807.
Kadereit, A., Greilich, S., Woda, C., Wagner, G.A., 2008. In: Reindel, M., Wagner, G.A. (Eds.), New Technologies for Archaeology, Natural Science in Archaeology. Springer-Verlag, Berlin Heidelberg. http://dx.doi.org/10.1007/978-3-540-87438-6_15, 2009.
Kadereit, A., Sponholz, B., Rösch, M., Schier, W., Kromer, B., Wagner, G.A., 2006. Chronology of Holocene environmental changes at the tell site of Uivar, Romania, and its significance for late neolithic tell evolution in the temperate Balkans. Z. für Geomorphol. N.F. 142, 19–45.
Kempe, S., al-Malabeh, A., 2010. Kites and other archaeological structures along the eastern rim of the harrat (Lava Plain) of Jordan, Signs of intensive usage in prehistoric time, a google earth images study. In: Proceedings of the 14th International Symposium on Vulcanospeleology, 2010, pp. 199–215.
Kempe, S., al-Malabeh, A., 2013. Desert kites in Jordan and Saudi Arabia: structure, statistics and function, a google earth study. Quat. Int. 297, 126–146.
Kennedy, D., 2011. The "Works of the old men" in arabia: remote sensing in interior arabia. J. Archaeol. Sci. 38, 3185–3203.
Kennedy, D., 2012. Editorial: wheels in the Harret al-Shaam. Palest. Explor. Q. 144, 77–81.
Kennedy, D., Banks, R., Houghton, P., 2014. Kites in Arabia. iBooks (Apple).
Kennedy, D.L., Bewley, R.H., 2009. Aerial archaeology in Jordan. Antiquity 83, 69–81.
Kennedy, D.L., Bishop, M.C., 2011. Google earth and the archaeology of Saudi Arabia. A case study from the Jeddah area. J. Archaeol. Sci. 38, 1284–1293.
Khresat, S.A., Qudah, E.A., 2006. Formation and properties of aridic soils of Azraq Basin in northeastern Jordan. J. Arid Enviorn. 64, 116–136.
Liritzis, I., 2011. Surface dating by luminescence: an overview. Geochronometria 38, 292–302.
Maitland, P., 1927. The "Works of the old men" in arabia. Antiquity 1, 197–203.
Mitchell, A., 2005. The ESRI Guide to GIS Analysis, vol. 2. ESRI Press p.252.
Murray, A.S., Wintle, A.G., 2000. Luminescence dating of quartz using an improved single-aliquot regenerative-dose protocol. Radiat. Meas. 32, 57–73.
Rees, L., 1929. The Transjordan desert. Antiquity 3, 389–407.
Rhodius, C., Kadereit, A., Siegel, U., Schmidt, K., Eichmann, R., Khalil, L.A., 2015. Constraining the time of construction of the irrigation system of Tell Hujayrat al-Ghuzlan near Aqaba, Jordan, using high-resolution optically stimulated luminescence (HR-OSL) dating. Archaeol. Anthropol. Sci. http://dx.doi.org/10.1007/s12520-015-0284-x.
Rink, W.J., Bartoll, J., 2005. Dating the geometric Nasca lines in the Peruvian desert. Antiquity 79, 390–401.
Roberts, R.G., Galbraith, R.F., Yoshida, H., Laslett, G.M., Olley, J.M., 2000. Distinguishing dose populations in sediment mixtures: a test of single grain optical dating procedures using mixtures of laboratory-dosed quartz. Radiat. Meas. 32, 459–465.
Rollefson, G.O., Rowan, Y.M., Wasse, A., 2010. Desert monuments to the dead: early pastoral's lifeways in Jordan's Eastern Desert. ACOR Newsl. 22.1.
Rollefson, G., Rowan, Y., Wasse, A., 2014. The late neolithic colonization of the eastern badia of Jordan. Levant 46. http://dx.doi.org/10.1179/0075891414Z.00000000046.
Rowan, Y.M., Rollefson, G.O., Wasse, A., Abu-Azizeh, W., Hill, A.C., Kersel, M.M., 2015a. The "land of conjecture": new late prehistoric discoveries at Maitland's Mesa and Wisad Pools, Jordan. J. Field Archaeol. 40, 176–189. http://dx.doi.org/10.1179/0093469015Z.000000000117.
Rowan, Y., Wasse, A., Rollefson, G., Kersel, M., Jones, M., Lorentzen, B., 2015b. Late neolithic architectural complexity at wisad pools, black desert. Neo-Lithics 1/15, 3–10.
Simms, A.R., Kouremenos, P., DeWitt, R., Drewry, A.M., 2011. A new approach to reconstructing sea levels in Antarctica using optically stimulated luminescence of cobble surfaces. Quat. Geochronol. 6, 50–60.
van den Bergh, S., 1992. The Nazca geoglyphs. An astronomical (?) mystery. Vistas Astron. 35, 273–280.
Vermeesch, P., 2009. RadialPlotter: a Java application for fission track, luminescence and other radial plots. Radiat. Meas. 44, 409–410.
Zeder, M.A., Bar-Oz, G., Rufolo, S.J., Hole, F., 2013. New perspectives on the use of kites in mass-kills of Levantine gazelle: a view from northeastern Syria. Quat. Int. 297, 110–125.